

# Advanced Exergy Analysis of the Flash Ironmaking Process

**Jannik Neumann, Frank Dammel, Peter Stephan**

*Institute for Technical Thermodynamics, Technical University of Darmstadt, Darmstadt, Germany,  
(neumann, dammel, pstephan)@ttd.tu-darmstadt.de*

## Abstract:

The growing demand for renewable energy highlights the importance of green energy carriers in mitigating the temporal and geographic imbalances between renewable energy supply and demand. Iron, as a metal fuel, offers a promising solution by enabling the storage of electrical energy from renewables through the thermochemical reduction of iron oxides with green hydrogen. This stored energy can be later converted back into electricity via thermochemical oxidation, such as in retrofitted coal-fired power plants. Transporting the iron/iron oxide in a closed cycle allows for spatial and temporal separation of renewable energy storage and release. To maximize the system efficiency of this energy-iron cycle, it is crucial to achieve high storage efficiencies during the thermochemical reduction of iron oxides. The flash ironmaking process is a promising method for this, as it allows for the reduction of fine iron oxide particles with green hydrogen without the need for pre- or post-treatment. Conventional exergy analyses, as well as advanced exergy analysis, are used to analyze the flash ironmaking process. The results reveal an exergetic system efficiency of 53.7% for a defined base case, with the largest share of exergy destruction attributed to unavoidable exergy destruction at 82.2% of the total exergy destruction. Additionally, most of the exergy destruction was endogenous at 89.4% of the total exergy destruction. These assessments indicate that the overall potential for improvement of the reduction plant is moderate, and component improvements should be prioritized over structural improvements to reduce avoidable endogenous exergy destruction.

## Keywords:

Direct Reduction of Iron; Exergy Analysis; Green Iron; Iron as Energy Carrier; Metal Fuels.

## 1. Introduction

The impact of climate change on both ecosystems and humans is becoming increasingly concerning, with approximately 3.3 to 3.6 billion people residing in highly susceptible areas [1]. Governments worldwide are facing the challenge of balancing electricity security and meeting the rising demand for electricity while simultaneously reducing emissions. This becomes even more challenging due to the recent global energy crisis triggered by Russia's invasion of Ukraine which highlights the vulnerability of the current energy system [2]. At the center of the required clean energy transition is the significant increase in renewable energy sources paired with the electrification of end-uses. However, due to the inherent variability of renewable energy sources, a secure and decarbonized power sector requires much larger-scale flexible resources than currently exist [3]. One cornerstone of future energy systems might be the use of carbon-free chemical energy carriers (ECs), which can convert clean electricity into stable media for energy storage and transport. By connecting various low-cost production regions with users of green ECs through global value chains, the future energy supply security can be ensured [3]. Iron is being considered as a potential alternative to frequently discussed ECs such as hydrogen and hydrogen-based ECs for the global transport and seasonal storage of renewable energy [4–7]. The energy-iron cycle consists of the storage of electrical energy via thermochemical reduction of iron oxides using green hydrogen, which can subsequently be converted back into electricity through thermochemical oxidation. This conversion process can take place in coal-fired power plants that have been retrofitted for this purpose [8]. This reuse of existing assets and infrastructure can lead to significantly reduced implementation times and costs compared to alternative ECs [7]. Furthermore, the transport and storage of iron/iron oxide is comparatively easy and does not require liquefaction or elevated pressures, which is an advantage over other ECs. The round trip efficiency and the cost of such an energy-iron cycle depend strongly on the regeneration (thermochemical reduction) of the iron oxides [7].

Thermochemical reduction of iron oxide is a well-established process that primarily utilizes coal in blast furnaces, resulting in a significant contribution of 7% to global CO<sub>2</sub> emissions [9]. However, an alternative method is to employ shaft furnace processes that use natural gas instead of coal, which offer a promising solution to reduce associated CO<sub>2</sub> emissions from ironmaking [9]. This approach is particularly useful in regions with access to cheap natural gas.

Among various routes towards carbon-neutral ironmaking, the shaft furnace process is considered the most promising due to its ability to operate with green hydrogen instead of natural gas and its comparatively high technological readiness level [10]. One drawback of the shaft furnace reduction process is the necessity of iron oxide pellets as feedstock, which must be prepared beforehand and adds to the costs and emissions (although the potential for carbon neutrality exists through the use of hydrogen or bio-mass [11]). Further processing is needed to obtain the required iron powder [8], typically by melting the reduced iron pellets in an energy-intensive electric arc furnace and subsequently water-atomizing the melt.

At the University of Utah a promising alternative technology called the flash ironmaking process [12, 13] has been developed, which can reduce energy consumption and capital investment requirements. This innovative process allows for the direct utilization of fine iron oxide particles without requiring additional pre- and post-treatment, eliminating the need for pelletization and iron powder production. The reaction rate is rapid, and residence times are short, typically just a matter of seconds [12, 14], compared to the minutes to hours required in shaft furnace reactors, thanks to the small particle size (ranging from 10 to 100 microns). The flash reactor reduction technology is a high-intensity process that is free from problems associated with operating at high temperatures, such as particle sticking, unlike other gas-based ironmaking processes that use fluidized bed or shaft furnace reactors. As a result, the process can be operated at elevated temperatures (i.e. above 1150 °C), resulting in a more intensive process. The flash ironmaking process offers several advantages, including dispensing with the requirement for pre- and post-treatment, low energy consumption and capital investment, and high-intensity. Given these advantageous features, the flash ironmaking process aligns perfectly with the described energy-iron cycle as a promising reduction process.

To improve the understanding, identify the sources of irreversibility, and estimate the real improvement potential of this energy-intensive process, exergy-based analyses are performed. For this purpose the methodology and process are described in detail before the analyses are performed.

## 2. Methodology

The flash ironmaking process will be analyzed using both conventional and advanced exergy analyses. These two analyses will be briefly summarized subsequently before the flash ironmaking process is described in more detail.

### 2.1. Exergy Analysis

An exergetic analysis is widely recognized as the most efficient method for evaluating the efficiency of energy conversion processes [15–17]. It provides insights by analyzing the real thermodynamic inefficiencies in a system and its components, which are not available by means of an energetic analysis. These can greatly enhance energy-intensive processes from a thermodynamic, an economic, and an ecological perspective. When evaluating systems that involve chemical reactions, the total specific exergy  $e_{\text{tot}}$  of a material stream, is a combination of both physical exergy  $e_{\text{ph}}$  and chemical exergy  $e_{\text{ch}}$ , as represented by

$$e_{\text{tot}} = e_{\text{ph}} + e_{\text{ch}} . \quad (1)$$

Physical exergy is calculated based on the current enthalpy  $h$  and entropy  $s$  as well as their reference state values ( $h_0$  and  $s_0$ ), using the following equation

$$e_{\text{ph}} = (h - h_0) + T(s - s_0) . \quad (2)$$

Chemical exergy, on the other hand, has two components: a reactive part, which is represented by the standard chemical exergies, and a non-reactive part due to mixing. This can be expressed as

$$e_{\text{ch}} = \sum_l \omega_l e_{\text{ch},l}^0 + T_0 \sum_l R_l x_l \ln(x_l) . \quad (3)$$

The standard chemical exergy  $e_{\text{ch},l}^0$  for each species  $l$  can be obtained from tables for standard reference environments [15, 18, 19] or it can be calculated for a process-specific reference environment. In this case, the latter approach is used, with the reference species being liquid  $\text{H}_2\text{O}$ ,  $\text{Fe}_2\text{O}_3$ , and ambient air. For iron and hydrogen, the standard chemical exergies based on the process-specific reference environment are  $6448 \text{ kJ kg}^{-1}$  and  $118246 \text{ kJ kg}^{-1}$ , respectively.

The exergy balance of a generic open control volume can be expressed by

$$\dot{E}_D = P + \dot{E}_Q + \sum_{in,i} \dot{m}_i e_{i,\text{tot}} - \sum_{out,j} \dot{m}_j e_{j,\text{tot}} - \dot{E}_L , \quad (4)$$

where  $\dot{E}_Q$  and  $P$  correspond to the time rates of exergy transfer associated to heat and work transfer, respectively. The exergy loss rate  $\dot{E}_L$  and exergy destruction rate  $\dot{E}_D$  depend on the chosen system boundary. For

this evaluation, the system boundaries extend into the environment with the constant reference temperature  $T_0$ . Therefore, any exergy reduction due to heat losses to the environment is considered as exergy destruction, and only the material streams leaving the system correspond to exergy losses. To determine the exergetic efficiency of a system or component, it is necessary to define a fuel (F) and a product (P) for the analyzed system or component. Then, the overall exergy balance can be expressed by

$$\dot{E}_D = \dot{E}_F - \dot{E}_P - \dot{E}_L, \quad (5)$$

where the definition of the product must be consistent with the purpose of the system/component. The exergetic efficiency is defined as the ratio of the rate of exergy transfer associated with the product to the rate of exergy transfer associated with the fuel

$$\epsilon = \frac{\dot{E}_P}{\dot{E}_F} = 1 - \frac{\dot{E}_D + \dot{E}_L}{\dot{E}_F}. \quad (6)$$

To compare the exergy destruction  $\dot{E}_{D,k}$  of individual components  $k$  and losses associated to material streams leaving the system  $\dot{E}_L$  to the total fuel exergy  $\dot{E}_{F,tot}$  of the overall system, exergy destruction  $y_{D,k}$  and exergy loss  $y_L$  ratios can be defined

$$y_{D,k} = \frac{\dot{E}_{D,k}}{\dot{E}_{F,tot}}, \quad y_L = \frac{\dot{E}_L}{\dot{E}_{F,tot}}. \quad (7)$$

This allows for the assessment of the relative contribution of each component to the total exergy destruction of the system and can be used to define the total exergetic system efficiency

$$\epsilon_{tot} = 1 - \sum_k y_{D,k} - y_L. \quad (8)$$

Conventional exergy analysis provides valuable insights into how energy systems can be improved, but it falls short in illustrating the impact of interactions among components within the overall system and the real potential (including technological limitations) for improvement [20, 21]. To overcome these limitations, advanced exergy analysis has been developed. This approach provides a more comprehensive view of the origin of exergy destruction, taking into account the interactions between components and offering a clearer picture of the potential for improvement.

## 2.2. Advanced Exergy Analysis

An advanced exergy analysis goes beyond conventional analysis by breaking down the exergy destruction within each component into its endogenous and exogenous parts, as well as its avoidable and unavoidable parts and their combinations. Determining the unavoidable and endogenous fractions of exergy destruction entails making certain discretionary judgments, and thus, is somewhat subjective. Nonetheless, the insights obtained from this division surpasses the drawbacks of partial subjectivity [22]. The methodology of advanced exergy analysis was developed at the Institute for Energy Engineering of Technical University Berlin [20–25] and will be briefly summarized before been applied to the flash ironmaking process.

### 2.2.1. Unavoidable and Avoidable Exergy Destruction

Although it may be possible to mitigate a fraction of the exergy destruction rate in a component, there is usually a residual amount that cannot be avoided due to a variety of limitations. These limitations can include techno-economic constraints such as material availability and cost, as well as thermodynamic restrictions. For instance, the maximum achievable efficiencies of turbo-machinery or electrolyzers may be limited by current or future technology, resulting in unavoidable exergy destruction. By segregating the exergy destruction into two distinct parts – unavoidable  $\dot{E}_{D,k}^{UN}$  and avoidable  $\dot{E}_{D,k}^{AV}$  – in the  $k^{\text{th}}$  component

$$\dot{E}_{D,k} = \dot{E}_{D,k}^{UN} + \dot{E}_{D,k}^{AV}, \quad (9)$$

a more precise evaluation of the potential to enhance the component's thermodynamic efficiency can be achieved. To estimate the value of  $\dot{E}_{D,k}^{UN}$  within each system component, the most favorable operating conditions that just cannot be achieved in the near future are assumed.

### 2.2.2. Endogenous and Exogenous Exergy Destruction

Additionally, the impact of interdependencies of the system component can be analyzed by separating the total exergy destruction within the  $k^{\text{th}}$  component into endogenous  $\dot{E}_{D,k}^{EN}$  and exogenous  $\dot{E}_{D,k}^{EX}$  parts

$$\dot{E}_{D,k} = \dot{E}_{D,k}^{EN} + \dot{E}_{D,k}^{EX}. \quad (10)$$

The endogenous share refers to the exergy destruction that takes place within the  $k^{\text{th}}$  component while all other components are ideal, and the component under assessment is performing at its designated efficiency. In contrast, the exogenous fraction represents the discrepancy between the overall exergy destruction and the endogenous exergy destruction for the specific component. Determining exogenous and endogenous exergy destruction values for individual components is a critical aspect of advanced exergy analysis. Traditionally, two methods, based on thermodynamic cycles and the engineering approach, have been employed [24]. However, these approaches have limitations such as computational difficulties, theoretical deficiencies, and the need for a large number of non-standard simulations, rendering them impractical [21, 25]. To overcome these limitations, a novel decomposition-based approach was recently developed [25] and successfully applied [26] by Penkuhn and Tsatsaronis. This method involves calculating the exogenous exergy destruction for a given component by applying a modified exergy balance equation

$$0 = \sum_j \dot{E}_{Q,j,k}^{\text{EN}} + P_k^{\text{EN}} + \sum_i (\dot{m}e)_{i,k}^{\text{EN}} - \sum_o (\dot{m}e)_{o,k}^{\text{EN}} - \dot{E}_{Dk}^{\text{EN}} \quad (11)$$

This equation takes into account the endogenous operation parameters, which include composition, pressure, temperature, mass flow rate, and exergy transfer to or from the components. It is crucial to define these endogenous parameters for each component in relation to the remaining idealized system. Additionally, the exergetic efficiency  $\epsilon_k$  of the component must be identical in both the endogenous case and the base case design. By using this novel approach, the drawbacks of previous methods can be avoided, providing a more accurate and practical solution to determine endogenous and exogenous exergy destruction values.

### 2.2.3. Combination of the Exergy Splitting Approaches

The combination of the two previous concepts results in the following equation for exergy destruction

$$\dot{E}_{D,k} = \dot{E}_{D,k}^{\text{UN,EN}} + \dot{E}_{D,k}^{\text{UN,EX}} + \dot{E}_{D,k}^{\text{AV,EN}} + \dot{E}_{D,k}^{\text{AV,EX}} \quad (12)$$

When optimizing a system based on the results of an advanced exergy analysis, it is important to focus on reducing the avoidable endogenous (that can be reduced by improving the efficiency of the component being considered) and avoidable exogenous (that can be reduced by changes to the system topology) exergy destruction. With these considerations in mind, the exergetic efficiency given in 6 can be adjusted

$$\epsilon_k^{\text{AV,EN}} = \frac{\dot{E}_{P,k}}{\dot{E}_{F,k} - \dot{E}_{D,k}^{\text{UN}} - \dot{E}_{D,k}^{\text{AV,EX}}} \quad (13)$$

Similarly to the differentiation of different parts of exergy destruction (see 12), the exergy destruction ratios can be further differentiated as follows

$$y_{D,k} = y_{D,k}^{\text{UN,EN}} + y_{D,k}^{\text{UN,EX}} + y_{D,k}^{\text{AV,EN}} + y_{D,k}^{\text{AV,EX}} \quad (14)$$

The important information is conveyed through the unavoidable, endogenous exergy destruction  $\dot{E}_{D,k}^{\text{UN,EN}}$ , which represents the smallest possible endogenous exergy destruction resulting from techno-economically constraints of the component as well as its interactions with other components [21, 26].

$$\dot{E}_{D,k}^{\text{UN,EN}} = \dot{E}_{D,k}^{\text{UN}} \frac{\dot{E}_{D,k}^{\text{EN}}}{\dot{E}_{D,k}} \quad (15)$$

The remaining different parts of exergy destruction can then be calculated by the introduced set of equations.

## 3. Flash Ironmaking

As previously mentioned the utilization of green hydrogen for green ironmaking is an emerging technology. This section provides a brief overview of the thermochemical reduction of iron oxides using hydrogen, followed by a detailed introduction to the flash ironmaking process.

### 3.1. Reduction of Iron Oxides with Hydrogen

The step-wise direct reduction of iron oxides with hydrogen at temperatures above 843 K proceeds through a series of intermediate stages, starting from hematite  $\text{Fe}_2\text{O}_3$ , then magnetite  $\text{Fe}_3\text{O}_4$ , followed by wüstite  $\text{Fe}_{(1-z)}\text{O}$ , and finally to metallic iron Fe [27]. The global reaction for the reduction of hematite is described by





To enable comparisons between energy-based and exergy-based analyses, a system efficiency parameter is defined, denoted as  $\eta_{\text{tot}}$ , for the given process. This parameter is calculated using the following equation

$$\eta_{\text{tot}} = \frac{\dot{m}_5 \cdot HV_5}{\sum_k P_k}, \quad (17)$$

where the numerator simply represents the product of the mass flow rate and the corresponding heating value of the product stream, and the denominator accounts for the sum of all energy supplied to the system.

The required definition of fuel and product for the exergy analyses, taking into account the splitting of chemical and physical exergy, for each component and at the system level is defined in Table 1. The unavoidable exergy destruction for each component is calculated individually at the component level, under the best conditions possible, to define the unavoidable exergy destruction. The technological limitations and associated assumptions are given in Table 2. For components where an exergetic efficiency cannot be defined (such as mixer 1 and the cyclone), as they do not serve any meaningful purpose from a thermodynamic perspective, the unavoidable exergy destruction is set equal to the endogenous exergy destruction. The same assumption was made for the flash reactor (consisting out of the combustor, mixer 2 and the reaction section). Another approach to defining unavoidable conditions for the flash reactor could be to assume full conversion ( $X = 1$ ) at the minimum possible hydrogen equivalence ratio. However, such an assumption would result in higher specific exergy destruction due to the inherent irreversibilities associated with the chemical reactions involved. Consequently, this approach would lead to negative avoidable exergy destruction, the interpretation of which is not clear.

To calculate the endogenous and exogenous exergy destruction, individual components with their corresponding exergetic efficiency are simulated in conjunction with an idealized system [25]. The real process takes into account factors such as incomplete conversion of iron oxides in the reactor, incomplete separation of water from the residual gaseous stream in the condenser, and a higher hydrogen equivalence ratio than thermodynamically required. In contrast, in the idealized process, full conversion is achieved ( $X = 1$ ), complete separation of water out of the recycle stream, and the minimal possible hydrogen equivalence ratio are assumed. The minimal hydrogen equivalence ratio  $\lambda_{\text{H}_2} = 2.6$  is obtained using chemical equilibrium calculation for the idealized system under the corresponding conditions ( $t = 1300^\circ\text{C}$ ,  $\omega_{\text{H}_2} = 57\%$ ,  $\omega_{\text{H}_2\text{O}} = 43\%$ ). These idealizations result in different mass flow rates and compositions. To ensure a fair comparison, the overall main product of the process is kept constant, corresponding in this case to the chemical exergy in stream 5 leaving the system ( $\dot{E}_{\text{ch},5} = 196.4\text{MW}$ ). Due to the full conversion and the corresponding higher specific chemical exergy of the product, the material flow is reduced to meet the same main product for both the idealized and real processes. To determine the endogenous exergy destruction within the air heater, we assume that the upstream air fan is operating isentropically and adjust the pressure accordingly, as pressure drops downstream should not be attributed to the air heater. The inlet of the hot stream is determined by the idealized reactor ( $X = 1$ ), while the approach temperature is adjusted to achieve the same exergetic efficiency as in the base case design. Similarly, the endogenous exergy destruction of the other heat exchangers are determined by using the streams of the idealized system and adjusting the approach temperature to achieve the same exergetic efficiency as in the base case design. For the reaction section and the combustor, the hydrogen equivalence ratio and the associated heat losses are adjusted to meet the same exergetic efficiency between the base case design and the idealized system in conjunction with the component, respectively. Since the reactor operates at atmospheric pressure, the pressure levels generated by the turbo-machinery are not required for the overall process and are associated with pressure drops in other components. Therefore, the entire exergy destruction within the turbo machinery is exogenous. The specifications for the calculation of endogenous exergy destruction and the resulting streams are given in Appendix B.

The results are derived using EBSILON<sup>®</sup> *Professional* [30] applying the thermodynamic data given in [28] and user defined routines for the calculation of physical and chemical exergies. The reference temperature and pressure is set to  $T_0 = 298.15\text{K}$  and  $p_0 = 1.013\text{bar}$ , respectively.

## 4. Results and Discussion

The energetic system efficiency of the base case design was determined to be  $\eta_{\text{tot}} = 61.7\%$  based on a conventional mass and energy-based analysis (not explicitly shown here). The energetic analysis identified the electrolyzer as the component with the highest losses, followed by the residual energy of the material streams leaving the system, and the heat losses of the combustor and heat exchangers. To get an impression of the achievable energetic system efficiency, the process was parameterized according to the assumed unavoidable technological constraints given in Table 2. This resulted in an energetic system efficiency of  $\eta_{\text{tot}} = 68.5\%$ , a significant improvement potential from the base case design.

Based on the conventional exergy analysis presented in Table 3, the exergetic system efficiency of  $\epsilon_{\text{tot}} = 53.7\%$  indicates significant inefficiencies within the process. The electrolyzer is responsible for the largest exergy de-

Table 1: Definition of fuel and product according to [29] for each component given in Fig. 1

Component	Fuel $\dot{E}_F$	Product $\dot{E}_P$
Electrolyzer	$P_{el} + \dot{E}_{15,ch} - (\dot{E}_{16,ph} + \dot{E}_{17,ph} - \dot{E}_{15,ph})$	$\dot{E}_{16,ch} + \dot{E}_{17,ch}$
Mixer 1	NA	NA
Hydrogen Preaheater	$\dot{E}_{6,ph} - \dot{E}_{7,ph}$	$\dot{E}_{11,ph} - \dot{E}_{10,ph}$
Combustor	$\dot{E}_{11,ch} + \dot{E}_{23,ch} - \dot{E}_{12,ch}$	$\dot{E}_{12,ph} - \dot{E}_{11,ph} - \dot{E}_{13,ph}$
Mixer 2	$\dot{m}_{12}(e_{12,ph} - e_{13,ph}) + (\dot{E}_{2,ch} + \dot{E}_{12,ch} - \dot{E}_{13,ch})$	$\dot{m}_{12}(e_{13,ph} - e_{2,ph})$
Flash Reactor	$\dot{E}_{13,ch} + \dot{E}_{13,ph} - \dot{E}_{3,ph}$	$\dot{E}_{3,ch}$
Cyclone	NA	NA
Air Heater	$\dot{E}_{4,ph} - \dot{E}_{5,ph}$	$\dot{E}_{20,ph} - \dot{E}_{19,ph}$
Air Fan	$P_{el}$	$\dot{E}_{19,ph} - \dot{E}_{18,ph}$
Iron Oxide Preheater	$\dot{E}_{20,ph} - \dot{E}_{21,ph}$	$\dot{E}_{2,ph} - \dot{E}_{1,ph}$
Condensate Pump	$P_{el}$	$\dot{E}_{15,ph} - \dot{E}_{14,ph}$
Cooling Water Pump	$P_{el}$	$\dot{E}_{25,ph} - \dot{E}_{24,ph}$
Recycle Compressor	$P_{el}$	$\dot{E}_{9,ph} - \dot{E}_{8,ph}$
Condenser	$\dot{E}_{7,ch} + (\dot{E}_{7,ph} - \dot{E}_{14,ph} - \dot{E}_{8,ph}) - (\dot{E}_{26,ph} - \dot{E}_{25,ph})$	$\dot{E}_{8,ch} + \dot{E}_{14,ch}$
Overall System	$\sum_k P_{el,k} + \dot{E}_{1,tot} + \dot{E}_{18,tot} + \dot{E}_{24,tot}$	$\dot{E}_{5,ch}$

Table 2: Technological assumptions for determination of avoidable and unavoidable exergy destruction

Component	Parameter	Base Case	Unavoidable Inefficiency
Pumps	Isentropic efficiency $\eta_{is}$	75 %	85 %
Compressors	Isentropic efficiency $\eta_{is}$	80 %	90 %
Condenser	Approach temp. $\Delta T$	10 K	1 K
Heat exchangers	Approach temp. $\Delta T$	50 K	3 K
Heat exchangers	Relative heat loss $Q_{rel,L}$	2.5 %	1 %
Electrolyzer	System efficiency $\eta_{LHV}$	70 %	74 %
Electric motors	Efficiency $\eta$	90 %	95 %

struction, followed by the condenser, hydrogen preheater, reactor, combustor, and the other heat exchangers. Figure 2 illustrates the exergy destruction ratios of all components, starting from the overall process fuel, in descending order leading to the defined product of the process. The analysis reveals that the turbo-machinery and the cyclone only cause insignificant exergy destruction. The exergy losses associated with streams leaving the system result in an exergy loss ratio of  $y_L = 1\%$ , with the chemical exergy of the oxygen leaving the system having the highest share. In contrast to the energetic analysis, which pointed to the material streams leaving the system, the exergy analysis quantifies the low quality of the energy within these streams due to the low associated temperatures. The exergetic efficiencies of the different components are mostly high, with the exception of the flash reactor, which suffers from the high inherent irreversibilities associated with the reduction reaction. Interestingly, the exergetic efficiency of the combustor is comparatively high, which is due to the partial oxidation and the high temperature of stream 11 entering the combustor.

Based on the analysis of unavoidable and avoidable exergy destruction, it is concluded that the total unavoidable and avoidable exergy destruction account for 82.2 % ( $\dot{E}_{D,tot}^{UN} = 136.1$  MW) and 17.8 % ( $\dot{E}_{D,tot}^{AV} = 29.4$  MW) of the exergy destruction, respectively. After factoring in the unavoidable exergy destruction, a modified exergetic efficiency of 85.8 % can be determined for the base case (cf. Table 3). The highest unavoidable exergy destruction is associated with the electrolyzer, the condenser, the flash reactor and the combustor, while the highest avoidable exergy destruction is related to the electrolyzer, the hydrogen preheater, the combustor and the iron oxide preheater. The share between endogenous and exogenous exergy destruction is even more one-sided, with endogenous exergy destruction accounting for 89.4 % and exogenous exergy destruction for 10.6 % of the total exergy destruction. These findings suggest that a large share of the exergy destruction is unavoidable. However, the assessments point out that improving individual components should have a higher priority over structural improvements.

When combining the two exergy splitting approaches, the total share of avoidable endogenous and avoidable exogenous exergy destruction in relation to the total avoidable exergy destruction is 87.1 % and 12.9 %, respectively. The electrolyzer, hydrogen preheater, and the combustor exhibit the highest potential for reducing endogenous avoidable exergy destruction. This highlights the potential for improvement through technological

Table 3: Results of conventional and advanced exergy analysis

Component	Conventional Exergy Analysis						Advanced Exergy Analysis				
	$\dot{E}_F$ [MW]	$\dot{E}_P$ [MW]	$\dot{E}_D$ [MW]	$\dot{E}_L$ [MW]	$\epsilon$ [-]	$y_D$ [-]	$\dot{E}_{D,k}^{UN,EN}$ [MW]	$\dot{E}_{D,k}^{UN,EX}$ [MW]	$\dot{E}_{D,k}^{AV,EN}$ [MW]	$\dot{E}_{D,k}^{AV,EX}$ [MW]	$\epsilon_k^{AV,EN}$ [-]
Electrolyzer	358.2	248.0	110.2	0.0	0.69	0.30	87.0	4.0	18.5	0.8	0.93
Condenser	460.7	449.0	11.7	0.0	0.97	0.0	7.8	3.5	0.2	0.1	1.00
Hydrogen Preheater	67.7	57.2	10.5	0.0	0.84	0.03	5.6	1.9	2.3	0.7	0.96
Flash Reactor	14.9	4.5	10.4	0.0	0.30	0.03	9.6	0.4	0.4	0.0	0.92
Combustor	53.4	43.2	10.2	0.0	0.81	0.03	5.5	2.0	2.0	0.7	0.96
Air Preheater	17.6	12.7	4.9	0.0	0.72	0.01	3.5	0.6	0.6	0.1	0.95
Iron Oxide Preheater	13.0	10.5	2.6	0.0	0.80	0.01	1.0	0.2	1.1	0.2	0.90
Mixer 2	80.9	78.3	2.6	0.0	0.97	0.01	1.8	0.4	0.4	0.1	1.00
Recycle Compressor	4.8	3.6	1.2	0.0	0.75	0.00	0.0	0.5	0.0	0.7	1.00
Cyclone	741.5	740.7	0.8	0.0	0.00	0.0	0.5	0.1	0.1	0.0	0.00
Air Fan	1.5	1.1	0.4	0.0	0.74	0.00	0.0	0.2	0.0	0.2	1.00
Mixer 1	0.0	0.0	0.0	0.0	0.00	0.00	0.0	0.0	0.0	0.0	0.00
Cooling Water Pump	0.0	0.0	0.0	0.0	0.67	0.00	0.0	0.0	0.0	0.0	1.00
Condensate Pump	0.0	0.0	0.0	0.0	0.68	0.00	0.0	0.0	0.0	0.0	1.00
Total	365.3	196.6	165.5	3.5	0.54	0.45	122.4	13.7	25.6	3.8	0.86*

\*) Exergetic system efficiency adjusted by the unavoidable parts:  $\epsilon_{tot}^{AV} = \frac{\dot{E}_{P,tot}}{\dot{E}_{F,tot} - \dot{E}_{D,tot}^{UN}}$

advances in water-electrolysis, heat recovery measures, and the importance of proper reactor design and operation, including internal combustion.

The exergy-based evaluations presented here demonstrate the potential for enhancement of the analyzed flash ironmaking process. While technological advancements in water-electrolysis and lower approach temperatures lead to obvious improvements in overall performance, it is evident that there is still potential for improvement of the flash reactor (sequence of combustor, mixer 2, and reaction section). The attained conversion and reaction conditions (reaction temperature, hydrogen equivalence ratio) result in exergy destruction upstream and downstream of the reactor, which could be reduced. However, it should be noted that although these assessments are thermodynamically correct, economic considerations remain the driving force in real-world process synthesis.

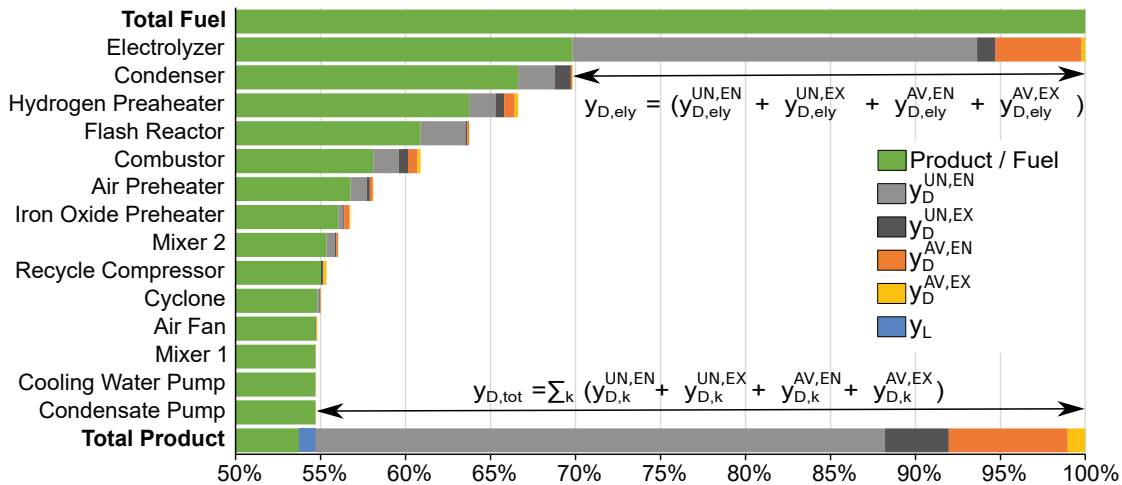


Figure 2: Waterfall diagram to visualize the results of the conventional and advanced exergy analysis

## 5. Conclusion

The present study focuses on the thermodynamic assessment of flash ironmaking, a promising method for sustainable iron oxide reduction using green hydrogen. To this end, conventional energy and exergy analyses, as well as an advanced exergy analysis, are conducted. A defined based case is used to determine an energetic efficiency of 61.7% and an exergetic efficiency of 53.7% for a given parameterization. For a scenario with foreseeable best case technological constraints, an energetic efficiency of 68.5% and an exergetic efficiency of 59.7% can be determined.

The informative value of the employed methods can be demonstrated by the assessment of the condenser, which separates the undesired water out of the recycle stream. While the energetic analysis points to the high energy content of the cooling water leaving the condenser, the exergetic analysis indicates significantly lower potential, which is further deemed as mainly unavoidable exergy destruction by the advanced exergy analysis. The overall potential for improvement of the plant is found to be moderate, mainly due to the high unavoidable exergy destruction (i.e. 82.2% of the total exergy destruction), and the improvement potential is primarily associated with the internal operational conditions of the components. The highest avoidable exergy destruction is observed in the electrolyzer, the hydrogen preheater, and the combustor, which is also endogenous. The findings of these analyses confirm that the flash ironmaking process is a promising alternative to the conventional shaft furnace process, particularly in the context of a circular energy-iron economy, given its dispensation of the requirement for pre- and post-treatment of iron oxides (required for the shaft furnace process), low energy consumption, and high-intensity. The performed assessments provide insights into the sources of irreversibility and estimate the potential for improvement in this energy-intensive process. However, for a more comprehensive assessment, it is crucial to consider economic factors in the synthesis of the analyzed flash ironmaking process. In addition to reliable techno-economic models, this requires a comprehensive reactor model that takes reaction kinetics and transport phenomena into account.

## Acknowledgments

The funding of the cluster project Clean Circles by the Hessian Ministry of Higher Education, Research, Science and the Arts is gratefully acknowledged.

## Appendix A Base Case Design

Table 4: Thermodynamic data for the base case design of the flash ironmaking process. Only selected mass fractions are shown. Missing fraction are obvious from the flow sheet (e.g. liquid water stream:  $\omega_{\text{H}_2\text{O}(l)} = 1$ ).

Stream	$\dot{m}$ [kg/s]	$p$ [bar]	$t$ [°C]	$e_{\text{tot}}$ [kJ/kg]	$e_{\text{ph}}$ [kJ/kg]	$e_{\text{ch}}$ [kJ/kg]	Mass Fractions $\omega_j$				
							Fe <sub>2</sub> O <sub>3</sub>	Fe	Fe <sub>0.947</sub> O	H <sub>2</sub>	H <sub>2</sub> O(g)
S1	48.0	1.01	25.0	0.0	0.0	0.0	1.00	0.00	0.00	0.00	0.00
S2	48.0	1.01	584.2	218.2	218.2	0.0	1.00	0.00	0.00	0.00	0.00
S3	59.4	1.01	1190.3	12490.9	1599.5	10891.5	0.00	0.49	0.10	0.06	0.35
S4	35.0	1.01	1190.3	6120.7	508.5	5612.1	0.00	0.83	0.17	0.00	0.00
S5	35.0	1.01	106.7	5617.0	4.9	5612.1	0.00	0.83	0.17	0.00	0.00
S6	24.4	0.91	1190.3	21610.0	3134.6	18475.4	0.00	0.00	0.00	0.16	0.84
S7	24.4	0.76	258.9	18830.8	355.4	18475.4	0.00	0.00	0.00	0.16	0.84
S8	5.7	0.61	25.0	78687.2	-433.1	79120.2	0.00	0.00	0.00	0.67	0.33
S9	5.7	1.16	99.4	79327.7	207.5	79120.2	0.00	0.00	0.00	0.67	0.33
S10	7.8	1.16	86.0	89667.0	196.3	89470.6	0.00	0.00	0.00	0.76	0.24
S11	7.8	1.01	1115.5	97029.7	7559.1	89470.6	0.00	0.00	0.00	0.76	0.24
S12	11.4	1.01	1598.8	65343.9	8957.2	56386.7	0.00	0.00	0.00	0.48	0.52
S13	59.4	1.01	1300.0	12666.8	1851.2	10815.6	0.81	0.00	0.00	0.09	0.10
S14	18.7	0.61	25.0	0.0	0.0	0.0	0.00	0.00	0.00	0.00	0.00
S15	18.7	1.16	25.0	0.0	0.0	0.0	0.00	0.00	0.00	0.00	0.00
S16	2.1	1.16	60.0	117722.0	196.9	117525.1	0.00	0.00	0.00	1.00	0.00
S17	16.6	1.16	60.0	134.6	12.4	122.1	0.00	0.00	0.00	0.00	0.00
S18	40.8	1.01	25.0	0.0	0.0	0.0	0.00	0.00	0.00	0.00	0.01
S19	40.8	1.35	56.7	26.3	26.3	0.0	0.00	0.00	0.00	0.00	0.01
S20	40.8	1.20	666.1	338.4	338.3	0.0	0.00	0.00	0.00	0.00	0.01
S21	40.8	1.05	130.3	18.5	18.5	0.0	0.00	0.00	0.00	0.00	0.01
S22	3.6	1.16	60.0	134.6	12.4	122.1	0.00	0.00	0.00	0.00	0.00
S23	13.0	1.16	60.0	134.6	12.4	122.1	0.00	0.00	0.00	0.00	0.00
S24	648.1	1.01	15.0	0.7	0.7	0.0	0.00	0.00	0.00	0.00	0.00
S25	648.1	1.20	15.0	0.7	0.7	0.0	0.00	0.00	0.00	0.00	0.00
S26	648.1	1.05	40.0	1.5	1.5	0.0	0.00	0.00	0.00	0.00	0.00

$$P_{\text{Ely}} = 358.82 \text{ MW}, P_{\text{AF}} = 1.46 \text{ MW}, P_{\text{CWP}} = 0.02 \text{ MW}, P_{\text{RC}} = 4.83 \text{ MW}, P_{\text{CP}} = 0.0 \text{ MW}$$

## Appendix B Calculation of Endogenous Exergy Destruction

Table 5: Thermodynamic data used for the calculation of endogenous exergy destruction. Only selected mass fractions are shown. Missing fraction are obvious from the flow sheet (e.g. liquid water stream:  $\omega_{\text{H}_2\text{O}(l)} = 1$ ).

Stream	$\dot{m}$ [kg/s]	$p$ [bar]	$t$ [°C]	$e_{\text{tot}}$ [kJ/kg]	$e_{\text{ph}}$ [kJ/kg]	$e_{\text{ch}}$ [kJ/kg]	Mass Fractions $\omega_j$				
							Fe <sub>2</sub> O <sub>3</sub>	Fe	Fe <sub>0.947</sub> O	H <sub>2</sub>	H <sub>2</sub> O(g)
<b>Air heater (AH):</b> $\epsilon_{\text{AH}} = 72.2\%$ , $T'_{19} = f(p'_{19}, \eta_{\text{is,AF}} = 1)$ , $p'_{19} = p_0 + \Delta p_{\text{AH}}$ , $T'_{20} = f(\epsilon_{\text{AH}})$ , $T'_5 = f(\epsilon_{\text{AH}})$											
S4	30.46	1.013	1175.5	6937.1	489.6	6447.4	0.00	1.00	0.00	0.00	0.00
S5	30.46	1.013	49.7	6447.9	0.4	6447.4	0.00	1.00	0.00	0.00	0.00
S19	37.02	1.163	36.9	12.1	12.1	0.0	0.00	0.00	0.00	0.00	0.01
S20	37.02	1.013	623.1	290.8	290.8	0.0	0.00	0.00	0.00	0.00	0.01
<b>Iron oxide preheater (IOPH):</b> $\epsilon_{\text{IOPH}} = 80.3\%$ , $T'_{20}, p'_{20} = p_0 + \Delta p_{\text{IOPH}}$ , $T'_2 = f(\epsilon_{\text{IOPH}})$ , $T'_{21} = f(\epsilon_{\text{IOPH}})$											
S1	43.55	1.01	25.0	0.0	0.0	0.0	1.00	0.00	0.00	0.00	0.00
S2	43.55	1.01	560.6	202.7	202.7	0.0	1.00	0.00	0.00	0.00	0.00
S20	37.02	1.16	641.0	316.3	316.3	0.0	0.00	0.00	0.00	0.00	0.01
S21	37.02	1.01	144.1	19.3	19.2	0.0	0.00	0.00	0.00	0.00	0.01
<b>Combustor (Comb):</b> $\epsilon_{\text{IOPH}} = 80.9\%$ , $e'_{11} = f(\lambda)$ , $e'_{12} = f(X, \lambda, T'_{12})$ , $m'_{22} = f(\lambda)$ , $m'_{11} = f(\lambda)$ , $T'_{12} = f(\epsilon_{\text{Comb}})$											
S11	4.63	1.01	1171.2	127713.5	10188.4	117525.1	0.00	0.00	0.00	1.00	0.00
S12	7.30	1.01	1644.2	79993.5	10821.7	69171.8	0.00	0.00	0.00	0.59	0.41
S22	2.67	1.01	60.0	123.9	1.7	122.1	0.00	0.00	0.00	0.00	0.00
<b>Flash Reactor (FR):</b> $\epsilon_{\text{FR}} = 30.2\%$ , $\lambda = f(\epsilon_{\text{FR}})$ , $e'_{13} = f(\lambda)$ , $e'_3 = f(\lambda)$											
S3	54.77	1.01	1154.6	9356.1	1270.4	8085.7	0.00	0.53	0.11	0.04	0.32
S13	54.77	1.01	1300.0	9539.2	1533.2	8006.0	0.88	0.00	0.00	0.07	0.06
<b>Cyclone (Cyc):</b> $\epsilon_{\text{Cyc}} = \text{NA}$ , $m'_3 = f(X, \lambda)$ , $T'_3 = T'_4 = T'_5$											
S3	51.43	1.01	1175.2	11332.5	1460.8	9871.7	0.00	0.59	0.00	0.05	0.36
S4	30.47	1.01	1175.2	6936.9	489.5	6447.4	0.00	1.00	0.00	0.00	0.00
S6	20.96	0.91	1175.2	17691.5	2843.8	14847.7	0.00	0.00	0.00	0.13	0.87
<b>Hydrogen Preaheater (HPH):</b> $\epsilon_{\text{HPH}} = 84.5\%$ , $T'_6, T'_7, p_{10} = p_0 + \Delta p_{\text{HPH}}$ , $p_6 = p_0$ , $T'_7 = f(\epsilon_{\text{HPH}})$ , $T'_{11} = f(\epsilon_{\text{HPH}})$											
S6	20.77	1.01	1173.3	17859.1	2875.0	14984.1	0.00	0.00	0.00	0.13	0.87
S7	20.77	0.86	272.3	15409.4	425.3	14984.1	0.00	0.00	0.00	0.13	0.87
S10	4.67	1.16	55.3	117715.3	190.2	117525.1	0.00	0.00	0.00	1.00	0.00
S11	4.67	1.01	1107.9	126920.9	9395.8	117525.1	0.00	0.00	0.00	1.00	0.00
<b>Condenser (Cond):</b> $\epsilon_{\text{Cond}} = 97.5\%$ , $T'_8 = T'_{14} = f(p'_8, \epsilon_{\text{cond}})$ , $p'_7 = p_0$ , $p'_8 = p_0 - \Delta p_{\text{Cond}}$											
S7	20.79	1.01	189.6	15319.2	349.9	14969.2	0.00	0.00	0.00	0.13	0.87
S8	3.12	0.91	16.0	99402.9	-108.9	99511.8	0.00	0.00	0.00	0.85	0.15
S14	17.68	0.91	16.0	0.6	0.6	0.0	0.00	0.00	0.00	0.00	0.00
S25	536.83	1.20	15.0	0.7	0.7	0.0	0.00	0.00	0.00	0.00	0.00
S26	536.83	1.10	40.0	1.5	1.5	0.0	0.00	0.00	0.00	0.00	0.00
<b>Electrolysis (Ely):</b> $\epsilon_{\text{Ely}} = 69.2\%$ , $P_{\text{Ely}} = 342.5 \text{ MW}$ , $T'_{15}, m'_{15} = f(X)$											
S15	17.87	1.01	16.0	0.6	0.6	0.0	0.00	0.00	0.00	0.00	0.00
S16	2.00	1.01	60.0	117552.1	27.1	117525.1	0.00	0.00	0.00	1.00	0.00
S17	15.87	1.01	60.0	123.9	1.7	122.1	0.00	0.00	0.00	0.00	0.00
<b>Mixer 2 (Mix2):</b> $\epsilon_{\text{Mix2}} = 96.8\%$ , $m_{12} = f(\lambda)$ , $e'_{12} = f(\lambda)$ , $T'_2$											
S2	43.56	1.01	618.3	241.8	241.8	0.0	1.00	0.00	0.00	0.00	0.00
S12	7.31	1.01	1639.1	81332.6	10918.9	70413.7	0.00	0.00	0.00	0.60	0.40
S13	50.86	1.01	1300.0	11849.3	1733.8	10115.5	0.86	0.00	0.00	0.09	0.06

## Nomenclature

$e$	specific exergy, $\text{J kg}^{-1}$
$\dot{E}$	time rate of exergy transfer, $\text{J s}^{-1}$
$h$	specific enthalpy, $\text{J kg}^{-1}$
$HV$	heating value, $\text{J kg}^{-1}$
$\dot{m}$	mass flow rate, $\text{kg s}^{-1}$
$N$	molar amount, mol
$P$	electrical/mechanical power, $\text{J s}^{-1}$
$R$	specific gas constant, $\text{J kg}^{-1} \text{K}^{-1}$
$s$	specific entropy, $\text{J kg}^{-1} \text{K}^{-1}$
$t$	temperature, $^{\circ}\text{C}$
$T$	temperature, K
$x$	mole fraction
$X$	reduction degree
$y$	exergy destruction/loss ratio

## Greek symbols

$\Delta$	difference
$\epsilon$	exergetic efficiency
$\eta$	efficiency
$\lambda$	hydrogen equivalence ratio
$\omega$	mass fraction

## Subscripts and superscripts

AV	avoidable
ch	chemical
D	destruction
el	electrical
EN	endogenous
EX	exogenous
Fe	iron
F	fuel
is	isentropic
L	loss
O	oxygen
ph	physical
P	product
Q	heat
rel	relative
tot	total
UN	unavoidable
0	standard, reference

## References

- [1] Pörtner, H.-O., D.C. Roberts, H. Adams, I. Adelekan, C. Adler, R. Adrian, P. Aldunce, E. Ali, R. Ara Begum, B. Bednar-. *IPCC, 2022: Summary for Policymakers*. 2022. URL: [https://www.ipcc.ch/report/ar6/wg2/downloads/report/IPCC\\_AR6\\_WGII\\_SummaryForPolicymakers.pdf](https://www.ipcc.ch/report/ar6/wg2/downloads/report/IPCC_AR6_WGII_SummaryForPolicymakers.pdf) (visited on Feb. 24, 2023).
- [2] IEA. *World Energy Outlook 2022*. URL: <https://iea.blob.core.windows.net/assets/830fe099-5530-48f2-a7c1-11f35d510983/WorldEnergyOutlook2022.pdf> (visited on Feb. 24, 2023).
- [3] IEA. *The role of low-carbon fuels in the clean energy transitions of the power sector*. 2022. URL: <https://iea.blob.core.windows.net/assets/01ca16c8-e493-475c-81c4-04ac5d3b9882/TheRoleoflow-carbonfuelsinthecleanenergytransitionsofthepowersector.pdf> (visited on Feb. 24, 2023).
- [4] Bergthorson J. M. *Recyclable metal fuels for clean and compact zero-carbon power*. In: *Progress in Energy and Combustion Science* 68 (2018), pp. 169–196. DOI: 10.1016/j.pecs.2018.05.001.
- [5] Debiagi P. et al. *Iron as a sustainable chemical carrier of renewable energy: Analysis of opportunities and challenges for retrofitting coal-fired power plants*. In: *Renewable and Sustainable Energy Reviews* 165 (2022), p. 112579. ISSN: 13640321. DOI: 10.1016/j.rser.2022.112579.
- [6] Kuhn C. et al. *Iron as recyclable energy carrier: Feasibility study and kinetic analysis of iron oxide reduction*. In: *Applications in Energy and Combustion Science* 12 (2022), p. 100096. ISSN: 2666352X. DOI: 10.1016/j.jaecs.2022.100096.
- [7] Neumann, J. and da Rocha, R. C. et al. *Techno-economic assessment of long-distance supply chains of energy carriers: Comparing hydrogen and iron for carbon-free electricity generation*. In: *Applications in Energy and Combustion Science* 14 (2023), p. 100128. DOI: 10.1016/j.jaecs.2023.100128.
- [8] Janicka J. et al. *The potential of retrofitting existing coal power plants: a case study for operation with green iron*. In: *Applied Energy* (2023). DOI: 10.1016/j.apenergy.2023.120950.

- [9] IEA. *Global crude steel production by process route and scenario, 2019-2050* –&nbsp;Charts – Data & Statistics - IEA. 2019. URL: <https://www.iea.org/data-and-statistics/charts/global-crude-steel-production-by-process-route-and-scenario-2019-2050> (visited on Feb. 9, 2023).
- [10] Suer J. et al. *Carbon Footprint and Energy Transformation Analysis of Steel Produced via a Direct Reduction Plant with an Integrated Electric Melting Unit*. In: Journal of Sustainable Metallurgy 8.4 (2022), pp. 1532–1545. ISSN: 2199-3823. DOI: 10.1007/s40831-022-00585-x.
- [11] Wiinikka H. et al. *Combustion Evaluation of Renewable Fuels for Iron-Ore Pellet Induration*. In: Energy & Fuels 33.8 (2019), pp. 7819–7829. ISSN: 0887-0624. DOI: 10.1021/acs.energyfuels.9b01356.
- [12] Sohn H. Y., Fan D.-Q., and Abdelghany A. *Design of Novel Flash Ironmaking Reactors for Greatly Reduced Energy Consumption and CO<sub>2</sub> Emissions*. In: Metals 11.2 (2021), p. 332. DOI: 10.3390/met11020332.
- [13] Sohn H. Y., Elzohiery M., and Fan D.-Q. *Development of the Flash Ironmaking Technology (FIT) for Green Ironmaking with Low Energy Consumption*. In: Journal of Energy and Power Technology 03.03 (2021), p. 1. ISSN: 26901692. DOI: 10.21926/jept.2103042.
- [14] Wang X. et al. *Numerical simulation of effect of operating conditions on flash reduction behaviour of magnetite under H<sub>2</sub> atmosphere*. In: International Journal of Hydrogen Energy 44.48 (2019), pp. 26261–26270. ISSN: 03603199. DOI: 10.1016/j.ijhydene.2019.08.089.
- [15] Kotas T. J. *The exergy method of thermal plant analysis*. Butterworths, 1985. ISBN: 9780408013505.
- [16] Bejan A., Tsatsaronis G., and Moran M. J. *Thermal design and optimization*. New York and Chichester: John Wiley, 1996. ISBN: 0471584673.
- [17] Tsatsaronis G. *Thermoeconomic Analysis and Optimization of Energy Systems*. In: Progress in Energy and Combustion Science 19 (1993), pp. 227–257. DOI: 10.1016/0360-1285(93)90016-8.
- [18] Ahrendts J. *Reference states*. In: Energy 5.8-9 (1980), pp. 666–677. ISSN: 0360-5442. DOI: 10.1016/0360-5442(80)90087-0.
- [19] Jan Szargut. *Towards an International Reference Environment of Chemical Exergy*. In: (2005). URL: <https://www.exergoecology.com/exergoecology/szargut2005> (visited on June 21, 2021).
- [20] Tsatsaronis G. and Morosuk T. *Understanding and improving energy conversion systems with the aid of exergy-based methods*. In: International Journal of Exergy 11.4 (2012), p. 518. ISSN: 1742-8297. DOI: 10.1504/IJEX.2012.050261.
- [21] Morosuk T. and Tsatsaronis G. *Advanced exergy-based methods used to understand and improve energy-conversion systems*. In: Energy 169 (2019), pp. 238–246. ISSN: 0360-5442. DOI: 10.1016/j.energy.2018.11.123.
- [22] Tsatsaronis G. et al. *Understanding the thermodynamic inefficiencies in combustion processes*. In: Energy 62 (2013), pp. 3–11. ISSN: 0360-5442. DOI: 10.1016/j.energy.2013.04.075.
- [23] Tsatsaronis G. *Recent developments in exergy analysis and exergoeconomics*. In: International Journal of Exergy 5.5/6 (2008), p. 489. ISSN: 1742-8297. DOI: 10.1504/IJEX.2008.020822.
- [24] Kelly S., Tsatsaronis G., and Morosuk T. *Advanced exergetic analysis: Approaches for splitting the exergy destruction into endogenous and exogenous parts*. In: Energy 34.3 (2009), pp. 384–391. ISSN: 0360-5442. DOI: 10.1016/j.energy.2008.12.007.
- [25] Penkuhn M. and Tsatsaronis G. *A decomposition method for the evaluation of component interactions in energy conversion systems for application to advanced exergy-based analyses*. In: Energy 133 (2017), pp. 388–403. ISSN: 0360-5442. DOI: 10.1016/j.energy.2017.03.144.
- [26] Penkuhn M. and Tsatsaronis G. *Comparison of different ammonia synthesis loop configurations with the aid of advanced exergy analysis*. In: Energy 137 (2017), pp. 854–864. ISSN: 0360-5442. DOI: 10.1016/j.energy.2017.02.175.
- [27] Spreitzer D. and Schenk J. *Reduction of Iron Oxides with Hydrogen—A Review*. In: steel research international 90.10 (2019), p. 1900108. ISSN: 1611-3683. DOI: 10.1002/srin.201900108.
- [28] McBride B. J., Zehe M. J., and Gordon S. *NASA Glenn Coefficients for Calculating Thermodynamic Properties of Individual Species*. 2002. URL: <https://ntrs.nasa.gov/citations/20020085330> (visited on Feb. 22, 2022).
- [29] Lazzaretto A. and Tsatsaronis G. *SPECO: A systematic and general methodology for calculating efficiencies and costs in thermal systems*. In: Energy 31.8-9 (2006), pp. 1257–1289. ISSN: 0360-5442. DOI: 10.1016/j.energy.2005.03.011.
- [30] Iqony GmbH. *EBSILON Professional*. URL: <https://www.ebsilon.com/en/> (visited on Mar. 14, 2023).